

Least-Squares Optimal Mismatched Doppler Processing

Lumumba A. Harnett and Shannon D. Blunt

Radar Systems Lab (RSL), University of Kansas, Lawrence, KS

Abstract—Doppler processing is a well-known tool for the discrimination of scatterers based on their rates of radial motion. It is part of nearly every kind of radar mode via the coherent combination of echoes from a set of pulses. While windowing is likewise a well-known approach to reduce Doppler sidelobes (which also incurs degraded resolution and SNR loss), here we leverage recent work on least-squares (LS) optimal mismatched filtering that employs over-sampling for high-fidelity along with the means to compensate for the attendant super-resolution degradation that would otherwise arise. The result is a mismatched Doppler processing (MMDP) transformation that reduces sidelobes with less SNR loss and resolution degradation than windowing, as demonstrated using simulation and free-space measurements.

Keywords—Doppler processing, clutter cancellation, least-squares

I. INTRODUCTION

Doppler processing stands as a cornerstone of modern radars that rely on relative radial motion to discriminate movers having different speeds, to identify and subsequently cancel stationary clutter [1, Chap. 17], and to enhance cross-range resolution for synthetic aperture radar (SAR) [2]. Each Doppler frequency can be represented by a specific frequency steering vector, such as is done for space-time adaptive processing (STAP) in combination with a spatial steering vector associated with the antenna array [3,4]. Alternatively, the complete Doppler spectrum can be readily obtained simply through application of the fast Fourier transform (FFT).

Because frequency steering vectors correspond to the relative temporal arrangement of pulses in a coherent processing interval (CPI), which usually involves uniform spacing of pulses so that an FFT can be used, the result of standard Doppler processing on receive would then realize high sidelobes in the Doppler domain. For this reason it is common to employ windowing of the frequency steering vectors to reduce these sidelobes, with the caveat that degraded resolution and signal-to-noise ratio (SNR) loss are consequently incurred [1, Chap. 14]. Examples of well-known windows for this purpose are Taylor, Hanning, Hamming, and Kaiser [5].

In contrast to windowing, here we consider a least-squares (LS) optimal mismatched Doppler processing (MMDP) transformation to replace standard Doppler processing. To do so we leverage recent modified forms of LS devised for pulse compression of frequency modulated (FM) waveforms [6,7] and stretch processing [8], where the signal model in each is over-sampled while steps are taken to prevent the degradation

that the attendant super-resolution effect would induce. It is shown that the resulting MMDP formulation in this context suppresses Doppler sidelobes with a minimal degree of loss due to mismatch effects. The end result, demonstrated both in high-fidelity simulation and with experimental free-space measurements, is a new tool that expands the trade-space of options for Doppler processing and the myriad radar modes that rely upon it. It is anticipated that this transformation, which depends on the specific structure of the CPI, could be particularly applicable to emerging waveform-diverse modalities (see [9]) where standard windowing may not be appropriate.

II. RECEIVED SIGNAL MODEL

Consider a radar receiving M pulses in a CPI. The received response from the illuminated scatterers and noise for the m th pulse can be expressed as

$$y(m, t) = \sum [s(t) * x(\omega, t)] e^{jm\omega} + v(m, t), \quad (1)$$

where $x(\omega, t)$ is the collection of scattering reflections induced by transmit waveform $s(t)$ as a function of normalized inter-pulse Doppler frequency ω , and $v(m, t)$ is additive noise. Pulse compression is performed as

$$z(m, t) = h(t) * y(m, t), \quad (2)$$

for $h(t)$ the match filter and neglecting the effect of intra-pulse Doppler. After discretization, the collection of M slow-time samples of the ℓ th range bin can be represented as a superposition of target scatterers (indexed by q_T), clutter patches (indexed by q_C), and noise via

$$\mathbf{z}(\ell) = \sum_{q_T} x_{q_T}(\ell) \mathbf{v}(\omega_{q_T}) + \sum_{q_C} x_{q_C}(\ell) \mathbf{v}(\omega_{q_C}) + \mathbf{v}(\ell), \quad (3)$$

where $\mathbf{v}(\omega_q)$ is an $M \times 1$ temporal steering vector corresponding to Doppler frequency ω_q , and with $x_{q_T}(\ell)$ and $x_{q_C}(\ell)$ the complex scattering of the targets and clutter patches, respectively. For a constant pulse repetition interval (PRI) over the CPI, the steering vector takes the usual Vandermonde form

$$\mathbf{v}(\omega) = [1 \quad e^{j\omega} \quad e^{j2\omega} \quad \dots \quad e^{j(M-1)\omega}]^T. \quad (4)$$

Doppler processing of the data represented by (3) can then be performed by applying the Doppler filter bank \mathbf{V} as

$$\hat{\mathbf{x}}_{\text{DP}}(\ell) = \mathbf{V}^H \mathbf{z}(\ell), \quad (5)$$

where $\mathbf{V} = [\mathbf{v}(-\pi) \ \mathbf{v}(-\pi + \Delta\omega) \ \mathbf{v}(-\pi + 2\Delta\omega) \ \cdots \ \mathbf{v}(+\pi)]$ is $M \times N$ for $K = N/M$ a Doppler over-sampling factor, Doppler granularity $\Delta\omega = 2\pi/N$, and $(\bullet)^H$ the Hermitian (complex-conjugate transpose) operation. Windowing of the data can be performed in conjunction with Doppler processing [1, Chap. 14] by replacing each vector \mathbf{v} in \mathbf{V} with the windowed vector $\tilde{\mathbf{v}} = \mathbf{v} \odot \mathbf{b}$, where \mathbf{b} is the window function (e.g. Taylor, Hamming, etc) and \odot is the Hadamard product. Of course, windowing also incurs degraded Doppler resolution and some degree of SNR loss. In the following we alternatively consider the formulation of a LS based optimal Doppler filter bank and then incorporate this optimal filter bank into adaptive clutter cancellation.

III. OPTIMAL MISMATCHED DOPPLER PROCESSING

The least-squares (LS) mismatch filter (MMF) was initially proposed in [10] as a means to suppress pulse compression range sidelobes for phase codes. More recently, this formulation was modified to enable the construction of an LS-MMF for arbitrary FM waveforms [6,7]. Because FM waveforms can possess a continuously changing phase (unlike phase codes that have a constant phase over a chip interval), this latter instantiation necessitates modest oversampling of the waveform relative to its 3-dB bandwidth along with subsequent “beamspoiling” to prevent an undesired super-resolution condition (where sidelobes are actually increased and a very high mismatch loss penalty is incurred).

The success of the LS-MMF for arbitrary FM waveforms [7,11,12] subsequently led to a related formulation for stretch processing in which the final fast Fourier transform (FFT) stage is replaced by an LS optimal transform that greatly reduces range sidelobes, has very little mismatch loss, and no resolution degradation [8]. Because the signal model and final stage of stretch processing can be expressed in a manner that is practically identical to (3) and (5), it stands to reason that Doppler processing could likewise make use of an optimal LS transformation.

Leveraging [8], define the $N \times N$ desired response matrix

$$\mathbf{D} = (\mathbf{V}^H \mathbf{V}) \odot \mathbf{E}, \quad (6)$$

where \mathbf{E} is an $N \times N$ banded Toeplitz matrix with ones on the main diagonal as well as on the $K - 1$ diagonals above and below the main diagonal. In contrast to a critically sampled case, in which $\mathbf{D} = \mathbf{I}$ (an identity matrix), the oversampled-by- K form in (6) provides the higher fidelity needed to suppress Doppler sidelobes with negligible loss in resolution and low SNR loss. To avoid the super-resolution that can arise from oversampling in this manner, the band of $2K - 1$ non-zero diagonals in \mathbf{D} represents the Doppler mainlobe response at the nominal resolution.

As in [8], the LS cost function for mismatched Doppler processing is likewise defined as

$$J_{\text{LS}} = \|\mathbf{U}_{\text{LS}}^H \mathbf{V} - \mathbf{D}\|_{\text{F}}^2 \quad (7)$$

for $\|\bullet\|_{\text{F}}$ the Frobenius norm. Taking the gradient of (7) with respect to \mathbf{U}_{LS} and setting the result equal to zero yields the

$M \times N$ optimal mismatched Doppler processing (MMDP) filter bank

$$\mathbf{U}_{\text{LS}} = (\mathbf{V}\mathbf{V}^H)^{-1} \mathbf{V}\mathbf{D}^H. \quad (8)$$

To avoid possible ill-conditioning effects, (8) can also be diagonally loaded as

$$\mathbf{U}_{\text{LS}} = (\mathbf{V}\mathbf{V}^H + \delta \mathbf{I}_{M \times M})^{-1} \mathbf{V}\mathbf{D}^H, \quad (9)$$

where δ is a positive scalar and $\mathbf{I}_{M \times M}$ is an identity matrix. The LS-based estimate of scattering after (non-adaptive) Doppler processing is thus obtained by

$$\hat{\mathbf{x}}_{\text{LS}}(\ell) = \mathbf{U}_{\text{LS}}^H \mathbf{z}(\ell). \quad (10)$$

For the special case in which $K = 1$ (thus $\mathbf{D} = \mathbf{I}$) and the matrix \mathbf{V} becomes an $M \times M$ discrete Fourier transform (DFT), then (8) simplifies to a scaled version of \mathbf{V} . It should also be noted that the particular structure of \mathbf{D} in (6) provides further control over the precise form that the LS filter in (8) and (9) can take. For example, Fig. 1 illustrates the magnitude and phase of a center column of \mathbf{D} when $K = 5$. Thus, in the same way that windowing trades off resolution for sidelobe reduction, one could expand the width or shape of the non-zero banded portion of \mathbf{E} in (6) to obtain even greater freedom in the realization of \mathbf{U}_{LS} .

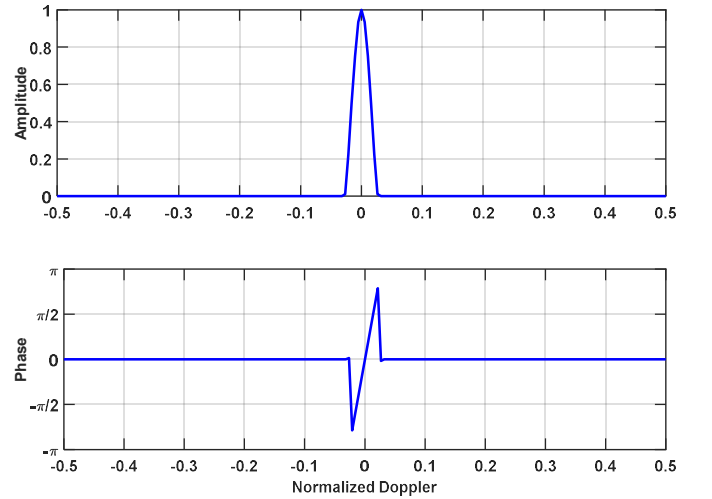


Fig. 1: Magnitude and phase of a center column of \mathbf{D} used in the least-squares formulation of the MMDP transform

IV. OPTIMAL MISMATCHED DOPPLER PROCESSING WITH INTERFERENCE CANCELLATION

In a moving target indication (MTI) scenario, the abundance of clutter in the radar scene can mask low-power, slow-moving targets. Adaptive clutter cancellation can be performed by applying the inverse of a clutter covariance matrix estimate $\hat{\mathbf{R}}(\ell)$ to the Doppler steering vectors in \mathbf{V} . In practice, the estimate of \mathbf{R} for a given cell under test (CUT) is generally obtained via the sample covariance matrix (SCM), which can be expressed as [4]

$$\hat{\mathbf{R}}(\ell_{\text{CUT}}) = \frac{1}{n(L)} \sum_{\ell \in L} \mathbf{z}(\ell) \mathbf{z}^H(\ell), \quad (11)$$

where L is the set of surrounding range cells excluding the CUT and an appropriate number of guard cells, and $n(L)$ is the cardinality of L . Thus the adaptive Doppler filter for the CUT is

$$\hat{\mathbf{W}}(\ell_{\text{CUT}}) = \hat{\mathbf{R}}^{-1}(\ell_{\text{CUT}}) \mathbf{V}, \quad (12)$$

which is itself dependent on range index ℓ . By collecting the windowed steering vectors $\tilde{\mathbf{v}} = \mathbf{v} \odot \mathbf{b}$ into the matrix $\tilde{\mathbf{V}}$, this matrix could replace \mathbf{V} in (12) to realize a windowed adaptive Doppler filter as well.

This same notion extends to the MMDP filter bank of (8) and (9). Specifically, a LS version of (12) can be defined as

$$\hat{\mathbf{W}}_{\text{LS}}(\ell_{\text{CUT}}) = \hat{\mathbf{R}}^{-1}(\ell_{\text{CUT}}) \mathbf{U}_{\text{LS}} \quad (13)$$

and subsequently applied as

$$\hat{\mathbf{x}}_{\text{LS, adap}}(\ell_{\text{CUT}}) = \hat{\mathbf{W}}_{\text{LS}}^H(\ell_{\text{CUT}}) \mathbf{z}(\ell_{\text{CUT}}). \quad (14)$$

In the following sections we compare the non-adaptive and adaptive MMDP filter banks to standard non-adaptive and adaptive Doppler processing, respectively.

Finally, a common metric for performance evaluation of adaptive interference cancellation is signal-to-interference-plus-noise ratio (SINR). Given clairvoyant knowledge of the covariance matrix \mathbf{R} , this metric [4,13] can be expressed in terms of mismatched Doppler processing as

$$\text{SINR}_{\mathbf{u}}(\omega) = \frac{|\mathbf{u}_{\text{LS}}^H(\omega) \mathbf{R}^{-1} \mathbf{v}(\omega)|^2}{\mathbf{u}_{\text{LS}}^H(\omega) \mathbf{R}^{-1} \mathbf{u}_{\text{LS}}(\omega)}. \quad (15)$$

Replacing \mathbf{u}_{LS} in (15) with $\tilde{\mathbf{v}}$ allows SINR to be evaluated in terms of windowed steering vectors as well. Likewise replacing \mathbf{u}_{LS} with \mathbf{v} simplifies to the usual form [4,13] of

$$\text{SINR}_{\mathbf{v}}(\omega) = \mathbf{v}^H(\omega) \mathbf{R}^{-1} \mathbf{v}(\omega). \quad (16)$$

V. SIMULATION RESULTS

Consider a linear FM waveform having a bandwidth of $B = 150$ MHz, a pulse duration of $T = 2 \mu\text{s}$, a fixed pulse repetition frequency (PRF) of 1 kHz, and $M = 38$ identical pulses in the CPI. Nonhomogeneous clutter [14] is modeled in the same manner as [13] by randomly modulating the power of each complex Gaussian range/angle clutter patch using a Weibull distribution with a shape parameter of 1.7 [15, 16]. The clutter is generated by dividing the range ring in azimuth into 39 ($> M = 38$) equal-sized clutter patches. The scattering from each patch is i.i.d. and drawn from a complex Gaussian distribution. Additive noise is also complex white Gaussian. Random internal clutter motion (ICM) is introduced that is uniformly distributed on $\pm 2\%$ relative to the normalized Doppler response. A Taylor window [17] is used that has $\bar{n} = 4$ nearly constant-level sidelobes adjacent to the mainlobe and a maximum sidelobe level of -30 dB.

For a given range cell, five targets are placed with different relative Dopplers and powers (the black x's in Figs. 2 and 3).

After pulse compression, Doppler receive processing is performed with oversampling $K = 5$ using the standard Fourier formulation of (5), a windowed version thereof using a Taylor window, and the LS MMDP per (8) and (10). The clairvoyant version of \mathbf{R} is used to assess clutter cancellation.

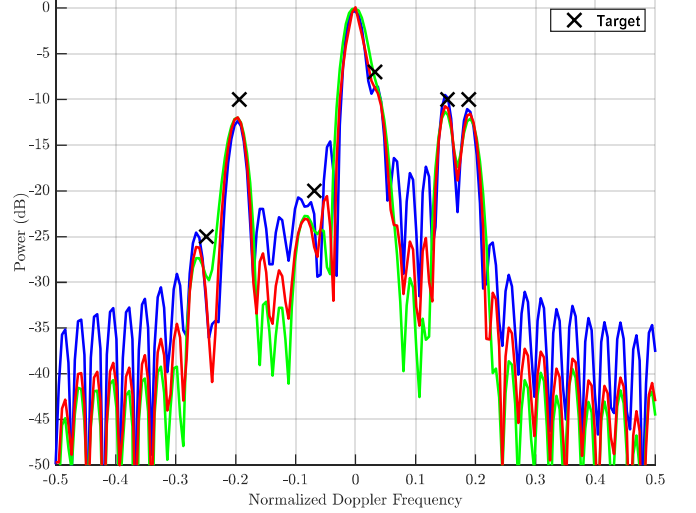


Fig. 2: Simulated Doppler processing spectrum before clutter cancellation for standard (blue), Taylor windowed (green), and MMDP (red)

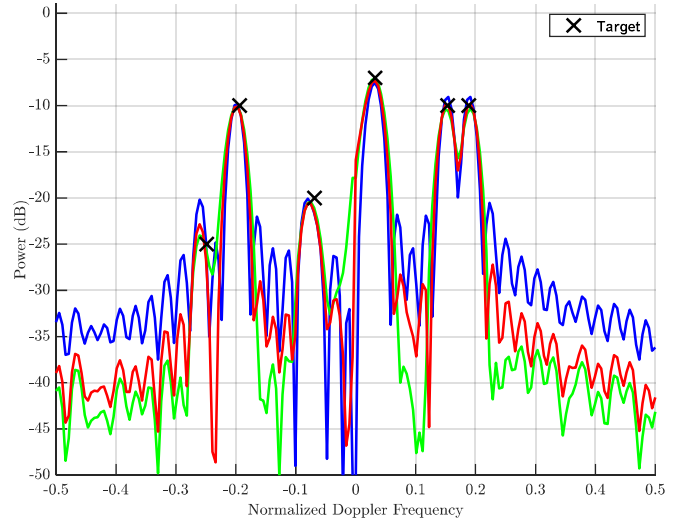


Fig. 3: Simulated Doppler processing spectrum after clutter cancellation for standard (blue), Taylor windowed (green), and MMDP (red)

Figure 2 illustrates an example of standard Doppler processing (blue), Taylor-windowed Doppler processing (green), and MMDP (red), where the large central peak corresponds to clutter. Figure 3 likewise shows the same set of responses after clutter cancellation. Close examination shows that MMDP provides slightly sharper peaks (particularly compared to the broadened peaks for Taylor windowing) and less SNR loss (particularly for smaller scatterers like the one at -0.25 normalized Doppler). While the MMDP sidelobes are not reduced to quite the same degree as Taylor windowing for

this basic operating mode, they are markedly lower than standard Doppler processing. In general, it has been found that while this Taylor window instantiation yields about 0.69 dB of loss, the MMDP in this case realizes only 0.27 dB.

In Figure 4, the SINR metric of (15) and (16) is shown for the three processing schemes based on clairvoyant knowledge of \mathbf{R} after 500 Monte Carlo trials. Here Taylor windowing incurs about 1.4 dB of SINR loss relative to standard processing, while MMDP only realizes about 0.5 dB. The clutter notch width is essentially unaffected.

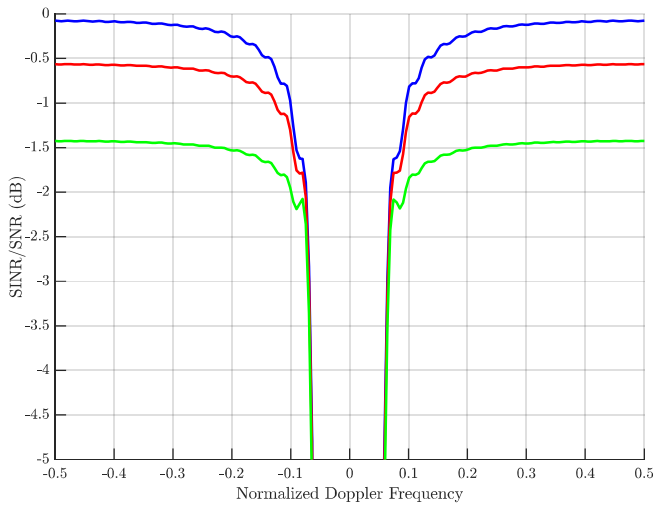


Fig. 4: Simulated clairvoyant SINR for standard (blue), Taylor windowed (green), and MMDP (red)

VI. OPEN-AIR EXPERIMENTAL RESULTS

Open-air experimental testing was performed at the University of Kansas using an LFM waveform of bandwidth $B = 150$ MHz, pulse duration $T = 2 \mu\text{s}$, and a fixed PRF of 100 kHz. In total, 4180 pulses were transmitted, with every 110 consecutive pulse echoes pre-summed in the receiver to yield an equivalent $M = 38$ pulses. The covariance matrix was estimated via (11) using $2M$ samples [18] and with 5 guard cells on either side of each CUT.

Figures 5-7 depict range/Doppler plots for the three approaches. Close inspection shows that, as expected, Taylor windowing (Fig. 6) reduces the Doppler sidelobes of standard processing (Fig. 5) while also broadening target mainlobe responses. The MMDP approach (Fig. 7) also reduces sidelobes, though to lesser degree than the Taylor window, but it also avoids the mainlobe spreading effect.

It is instructive to consider the Doppler cut at a single range for these results. Figures 8 and 9 show the measured Doppler spectrum of the three approaches before and after clutter cancellation, respectively. Like the simulated results in Figs. 2 and 3, it is again observed that MMDP has lower sidelobes than standard Doppler processing, but not quite as good as Taylor windowing. However, at +10 m/s appears to be a small moving target (most likely a motorcycle) for which the Taylor windowed response is clearly lower than that of MMDP. The stationary clutter at 0 m/s and the large moving target at +6 m/s

(likely a large truck) also show the greater spreading of the Taylor window implementation relative to standard or MMDP approaches.

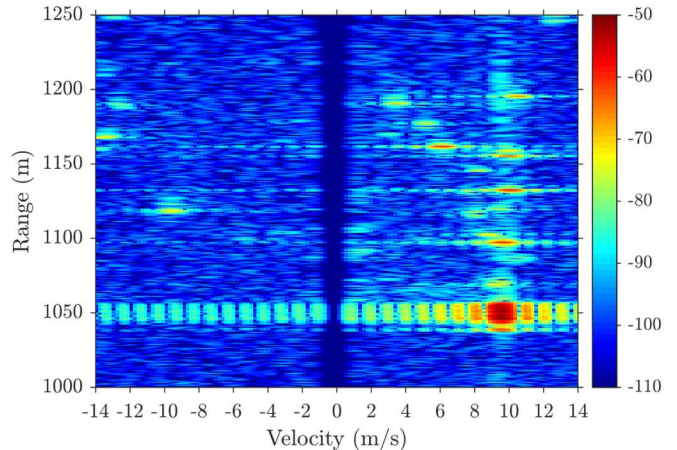


Fig. 5: Standard Doppler processing with clutter cancellation for open-air measurements

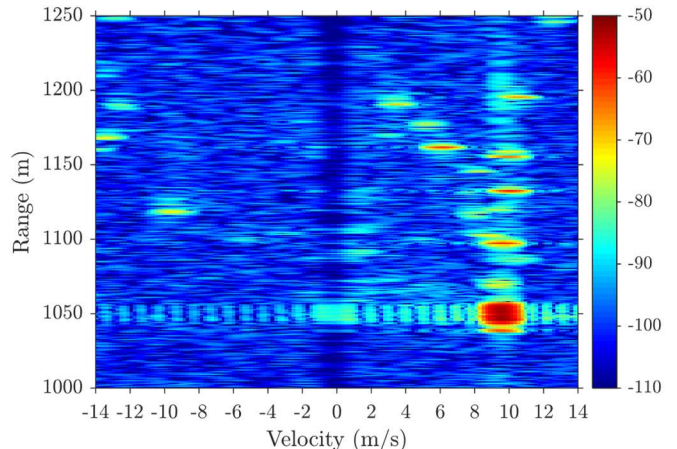


Fig. 6: Taylor windowed Doppler processing with clutter cancellation for open-air measurements

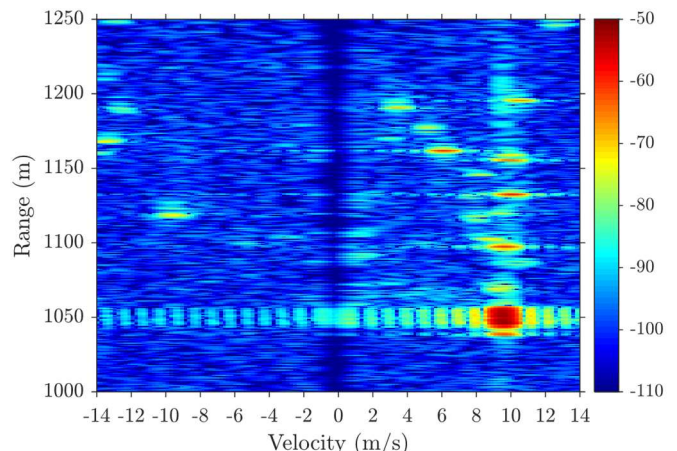


Fig. 7: MMDP with clutter cancellation for open-air measurements

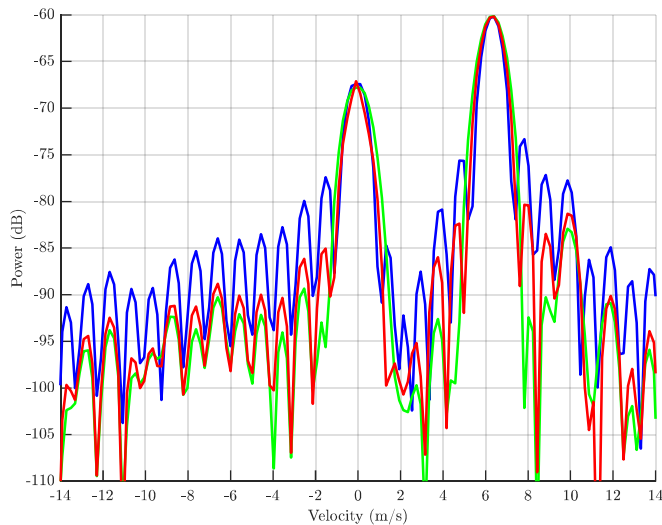


Fig. 8: Open-air measured Doppler spectrum before clutter cancellation at 1.167 km for standard (blue), Taylor windowed (green), and MMDP (red)

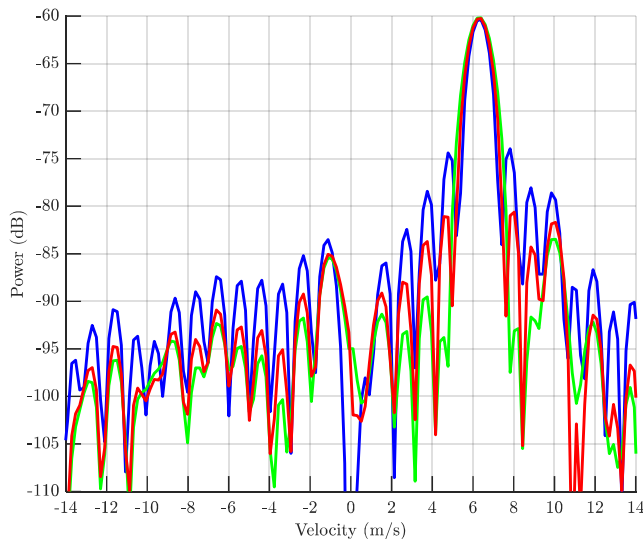


Fig. 9: Open-air measured Doppler spectrum after clutter cancellation at 1.167 km for standard (blue), Taylor windowed (green), and MMDP (red)

VII. CONCLUSIONS

A form of least-squares (LS) mismatch filtering, recently developed for pulse compression of FM waveforms and optimal stretch processing, has been formulated for use in Doppler processing. Simulated and experimentally measured results indicate that mismatched Doppler processing (MMDP) can reduce Doppler sidelobes, albeit not quite as much as Taylor windowing, while incurring less SNR loss due to mismatch.

The main purpose of this work was to illustrate that this manner of Doppler processing is indeed viable in practice. While the results thus far are by no means groundbreaking, this formulation sets the stage for new approaches to windowing (via modification of the desired \mathbf{D} matrix in the LS

formulation), greater control over mismatch loss through the diagonal loading term in (9), and as a potential robust way in which to reduce Doppler sidelobes when a non-uniform PRI is employed. Ongoing work is exploring the efficacy of these attributes.

REFERENCES

- [1] M.A. Richards, J.A. Scheer, W.A. Holm, *Principles of Modern Radar: Basic Principles*, SciTech Publishing, 2010.
- [2] W.L. Melvin, J.A. Scheer, *Principles of Modern Radar: Advanced Techniques*, SciTech Publishing, 2013.
- [3] R. Klemm, *Space-Time Adaptive Processing: Principles and Applications*. IEE Radar, Sonar, Navigation, and Avionics, 1998.
- [4] W.L. Melvin, "A STAP overview," in *IEEE Aerospace and Electronic Systems Magazine*, vol. 19, no. 1, pp. 19-35, Jan. 2004.
- [5] F.J. Harris, "On the use of windows for harmonic analysis with the discrete Fourier transform," *Proc. IEEE*, vol. 66, no. 1, pp. 51-83, Jan. 1978.
- [6] S.D. Blunt, M. Cook, J. Jakabosky, J. de Graaf, E. Perrins, "Polyphase-coded FM (PCFM) radar waveforms, part I: implementation," *IEEE Trans. Aerospace & Electronic Systems*, vol. 50, no. 3, pp. 2218-2229, July 2014.
- [7] D. Henke, P. McCormick, S.D. Blunt, T. Higgins, "Practical aspects of optimal mismatch filtering and adaptive pulse compression for FM waveforms," *IEEE Intl. Radar Conf.*, Arlington, VA, May 2015.
- [8] L. Harnett, D.M. Hemmingsen, P.M. McCormick, S.D. Blunt, C. Allen, A. Martone, K. Sherbondy, D. Wikner, "Optimal and adaptive mismatch filtering for stretch processing," *IEEE Radar Conf.*, Oklahoma City, OK, Apr. 2018.
- [9] S.D. Blunt, E.L. Mokole, "An overview of radar waveform diversity," *IEEE AESS Systems Magazine*, vol. 31, no. 11, pp. 2-42, Nov. 2016.
- [10] M.H. Ackroyd, F. Ghani, "Optimum mismatched filters for sidelobe suppression," *IEEE Trans. Aerospace & Electronic Systems*, vol. AES-9, no. 2, pp. 214-218, Mar. 1973.
- [11] J. Jakabosky, S.D. Blunt, B. Himed, "Spectral-shape optimized FM noise radar for pulse agility," *IEEE Radar Conf.*, Philadelphia, PA, May 2016.
- [12] C. Sahin, J. Metcalf, S. Blunt, "Filter design to address range sidelobe modulation in transmit-encoded radar-embedded communications," *IEEE Radar Conf.*, Seattle, WA, May 2017.
- [13] S.D. Blunt, J. Metcalf, J. Jakabosky, J. Stiles, B. Himed, "Multi-waveform space-time adaptive processing," *IEEE Trans. Aerospace & Electronic Systems*, vol. 53, no. 1, pp. 385-404, Feb. 2017.
- [14] W. L. Melvin, "Space-time adaptive radar performance in heterogeneous clutter," *IEEE Trans. Aerospace & Electronic Systems*, vol. 36, no. 2, pp. 621-633, Apr. 2000.
- [15] J.B. Billingsley, A. Farina, F. Gini, M.V. Greco, L. Verrazzani, "Statistical analyses of measured radar ground clutter data," *IEEE Trans. Aerospace & Electronic Systems*, vol. 35, no. 2, pp. 579-593, Apr 1999.
- [16] J.G. Metcalf, K.J. Sangston, M. Rangaswamy, S.D. Blunt, B. Himed, "A new method of generating multivariate Weibull distributed data," *IEEE Radar Conf.* Philadelphia, PA, USA, May 2016.
- [17] T. T. Taylor, "Design of line-source antennas for narrow beamwidth and low side lobes," in *Transactions of the IRE Professional Group on Antennas and Propagation*, vol. 3, no. 1, pp. 16-28, Jan. 1955
- [18] I. S. Reed, J. D. Mallett and L. E. Brennan, "Rapid Convergence Rate in Adaptive Arrays," in *IEEE Transactions on Aerospace and Electronic Systems*, vol. AES-10, no. 6, pp. 853-863, Nov. 1974.